Theoretical study of different attenuation measurement by acoustic microscopy

F. Hamdi,[1,a)] S. Bouhedja,[1,2] and H. Amrani[1]
[1]*Laboratoire Hyperfréquences et Semiconducteurs, département d'Electronique, Faculté des Sciences et de la technologie, université de Constantine1, BP 325 Route Ain El Bey, Constantine 25017, Algeria*
[2]*Département de Médecine, Faculté des Sciences Médicales, Université de Constantine3, BP125 Chalet des pins, Constantine 25000, Algeria*

(Received 29 March 2013; accepted 16 September 2013; published online 1 October 2013)

Many works are devoted to study the attenuation of surface waves in media, particularly, leaky surface acoustic waves (LSAW). In this work, a big part of the study is based on the intensity of the output signal, i.e., acoustic signature, V(z). The latter is obtained by the use of quantitative mode of acoustic microscopy in order to measure the velocity and the attenuation of those excited waves at the limit between the specimen and the coupling liquid. Our aim is to compare the attenuation values of the LSAW propagation in porous silicon obtained with three different methods. The first is obtained by resolving Viktorov equation. The second method is the spectral analysis acoustical signature V(z) curves. The third method uses the dark field. The obtained results are in a good agreement with those experiments. © *2013 AIP Publishing LLC*. [http://dx.doi.org/10.1063/1.4823850]

I. INTRODUCTION

The attenuation allows the evaluation of many important acoustic properties for the sample. Because of the mechanical properties and material structure, the incident wave emitted by the sensor will be differently attenuated during their propagation on the sample surface. In fact, those waves will lose their energy under the effect of absorption, induced diffusion in the presence of dislocations, micro-cracks, grain joints, etc., The measured attenuation from the acoustical signature reflects both the efficiency of wave's reemission in coupling liquid and the attenuation of the wave on the media surface. Therefore, the non-destructive technique of scanning acoustic microscopy[1–3] based on the emission and reflection of acoustic waves is a well-used tool and still promising in the attenuation investigations. Many methods are proposed to measure the attenuation coefficient[4–6] by determining the output signal V(z) detected by the transducer, versus sample defocusing z. The main tool is the scanning acoustic microscope (SAM) that is still interesting to study media characteristics.[7] It uses, in quantitative mode, the amplitude of output signal, i.e., acoustic signature, V(z), modeled by Sheppard and Wilson in function of lens's pupil function, the angle between the wave number and the lens axis, and the reflection coefficient.[8]

In this work, we use three different methods to calculate attenuation coefficient of surface acoustic waves in porous silicon samples (PSi). This material has gained a lot of interest because of its optical, electrical, and mechanical properties. The latter has been studied on both theoretical and experimental levels,[9–11] in particular, Young's modulus and the longitudinal and transverse velocities. They have been measured according to the porosity as well as the micromorphology with frequencies up to some GHz for thorough structural studies.[12,13] For the theoretical work using the quantitative method of the acoustic microscopy, calculations have been applied to a bulk and isotropic structure of PSi. The first method used is obtained by resolving Viktorov equation.[4] The second method is the spectral analysis of the acoustic signature curves.[5] The third method uses the dark field.[6] In order to perform numerical simulations, focus was given to the effect of the porosity and frequency on the attenuation of Rayleigh waves propagating in PSi. We have therefore used the laws established in Refs. 14–16 to write the dependence of longitudinal, V_{LP}, and transverse, V_{IP}, velocities and porosity, P, as

$$V_{LP} = V_{L0}(1 - P)^{1.095}, \quad (1)$$

$$V_{TP} = V_{T0}(1 - P)^{1.19}, \quad (2)$$

where the index notation "0" is used to indicate the value for bulk Si. Assuming that the coupling liquid does not penetrate into PSi, density is then given by

$$\rho = \rho_0(1 - P). \quad (3)$$

The calculations were performed using the normal operating state of simulation of a scanning acoustic microscope operating in reflection mode: operating frequency is 600 MHz, a half opening angle of 50°, and water of velocity $(V_{liq}) = 1500\,m/s$ as the liquid coupling and density $(\rho_{liq}) = 1000\,kg/m^3$. For bulk silicon, the density is $\rho_0 = 2330\,kg/m^3$, the longitudinal V_{L0} and transverse V_{T0} velocities are, respectively, 8570 m/s and 5840 m/s. We note that those conditions are favorable in Rayleigh mode excitation, which is the most dominant mode until 45% of porosity from which the dominance returns to longitudinal mode.

a)Author to whom correspondence should be addressed. Electronic mail: f_7amdi@yahoo.fr

II. METHODOLOGY

In many previous publications,[2,6,17] studies have focused on the calculation of the attenuation coefficient. In this section, we describe three different methods for our calculations.

A. Analytical method

The propagation characteristics of leaky surface acoustic waves represent the solution of the Viktorov equation[4]

$$4K^2[(K^2 - K_l^2)(K^2 - K_t^2)]^{1/2} - (2K^2 - K_t^2)^2 - jK_t^4(\rho_{liq}/\rho)\,[(K^2 - K_l^2)/(K_{liq}^2 - K^2)]^{1/2} = 0, \quad (4)$$

where

$$K_l = \omega/V_L, \quad K_t = \omega/V_T, \quad \text{and} \quad K_{liq} = \omega/V_{liq}.$$

K_t, K_l, and K_{liq} are, respectively, transverse, longitudinal, and coupling liquid wave vectors. ω is the angular frequency and equal to $2\pi f$.

K, the complex wave vector, gives the solution K_{Lsaw} for leaky surface acoustic waves (LSAW) mode, which is defined by the following equation:

$$K_{LSAW} = \frac{\omega}{V_{LSAW}}(1 + j\alpha_N), \quad (5)$$

where V_{LSAW} and α_N are the velocity and the normalized attenuation coefficient, respectively. The solution of Eq. (4) is obtained numerically.

B. Method of spectral analysis

The spectral analysis method was first proposed by Kushibiki.[5,18] It was introduced to analyze from the curves of the acoustic signature V(z) two acoustic quantities, i.e., the velocity and attenuation. By applying the Fourier transform FFT on the curves V(z), the velocity is determined from a center frequency, which is given by a maximum spectrum, while the attenuation is determined from the distribution of the spectrum.

Our simulation requires to follow of the following steps: (i) calculation of the acoustic signature V (z), (ii) subtracting from V(z) the lens response VL(z), (iii) applying FFT to the signal $V_{PSi}(z) = V(z)–VL(z)$, (iv) determining the period Δz from the principal ray of the FFT spectrum, (v) calculating the velocity of propagation of the considered mode, and finally, (vi) determining the attenuation coefficient, α_0, from the spectrum distribution.[5] Depending on acoustic radiation model,[19] the attenuation factor α_0 is related to two attenuation factors: the first is the leaky waves α_R on the water/PSi interface. The second is the braking of the longitudinal wave in water α_{Liq}[20] and can be written as

$$\alpha_R = \frac{\alpha_0}{2\tan\theta_R} + \frac{\alpha_{Liq}}{\sin\theta_R}. \quad (6)$$

Generally, in the presentation of results, we use the normalized attenuation,[6,14,21] a parameter that eases the comparison of results. It is given by

$$\alpha_N = \frac{\alpha_R V_R}{2\pi f}. \quad (7)$$

C. Dark field Method

In the literature,[6,20,21] the method of dark field is used to study the attenuation of Rayleigh wave modes. It is manifested in the calculation and the analysis of the curves V(z) obtained by using a SAM of reflection with annular lenses of varying diameters. Therefore, the methodology is to cover, with an absorbent material of circular shape, the central part of the lens. By calculating R(θ) and V(z) for each occulted angle θ_{occ}, we determine the attenuation of the Rayleigh wave from the exponential decay of interference curves V(z) obtained by using annular lenses.

III. RESULTS AND DISCUSSION

The importance of this investigation lies on the direct determination of porous silicon acoustic parameters of any value of the porosity. Experimental research conducted so far on porous silicon[14,22] shows that the variation of the longitudinal and transverse velocities is inversely proportional to the porosity. This result is of a great importance in this study. It has allowed us to deeply study the structure of the material.

A. Simulation of the acoustic signature V(z)

The interference phenomenon in the curves of V(z) can be associated with multiple leaky waves, such as surface acoustic waves, skimming longitudinal waves, harmonic modes of leaky waves, etc. In general, only the most important mode appears in the curves of V(z) and dominates all others. Thus, the response of the signal is due to the interface of a narrow packet of reflected axial waves and Rayleigh waves excited on the surface at a given angle of incidence θ_R.

Figure 1(a) shows, on one hand, the curves of the acoustic signature V versus the object-lens defocusing z, obtained by the theoretical simulation of water/porous silicon structure, PSi, for different values of porosity. We note that as long as the porosity increases, the oscillation period decreases. This quantitative analysis is confirmed by the decrease in Rayleigh velocity. Note that the values obtained by our simulation are comparable to experimental results cited in the literature.[14]

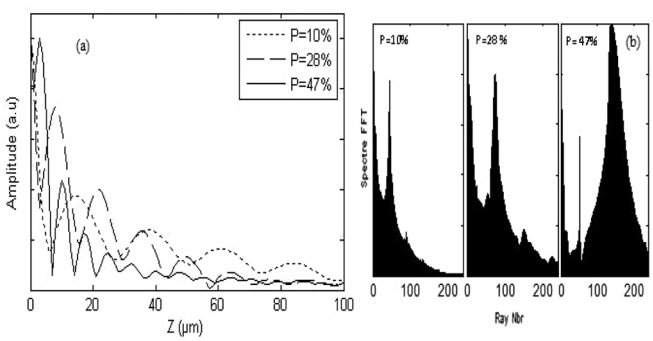

FIG. 1. Acoustic signatures: (a) and spectrum (b) for different porosity rates.

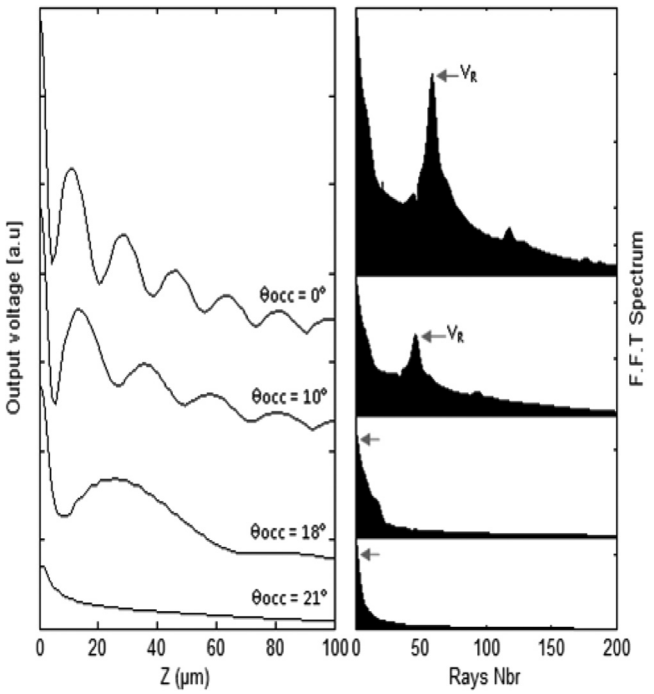

FIG. 2. Evolution of acoustic signatures versus the defocusing and their FFT spectrum for water/PSi structure for different occultations at 20% porosity.

These values are confirmed by Fig. 1(b) that shows the FFT spectrum. We find that the more porosity increases, the more the peak, which represents the Rayleigh mode, shifts to values of lower velocities.

Using the method of dark field and fixing the value of the porosity, we are interested in curves with maximum decay, that is to say those without oscillations. These curves are the result of maximum occultation where the interference phenomenon disappears and the amplitude of acoustic signatures oscillations tends to decrease exponentially.

Figure 2 illustrates the acoustic signatures of water/PSi structure for a porosity of 20%, obtained at different occultation angles, θ_{occ}. As well as the expansion of acoustic signatures' period and the displacement of the main peak ray indicating the Rayleigh mode in the FFT spectrum were also observed for this structure.

B. Attenuation coefficient

To illustrate the effect of porosity on wave attenuation using the three methods, we are interested in the study of the normalized attenuation coefficient. For its determination, we used an optimization method for adjusting the curve V(z) by an appropriate mathematical function of the form $\alpha_N = \alpha_{N0} \exp(b_N P)$. The values of the constants listed for the three methods are cited in Table I.

TABLE I. Obtained values for the three methods.

	Method 1	Method 2	Method 3
α_{N0}	0.0231	0.0204	0.0215
b_N	2.994	3.319	3.174

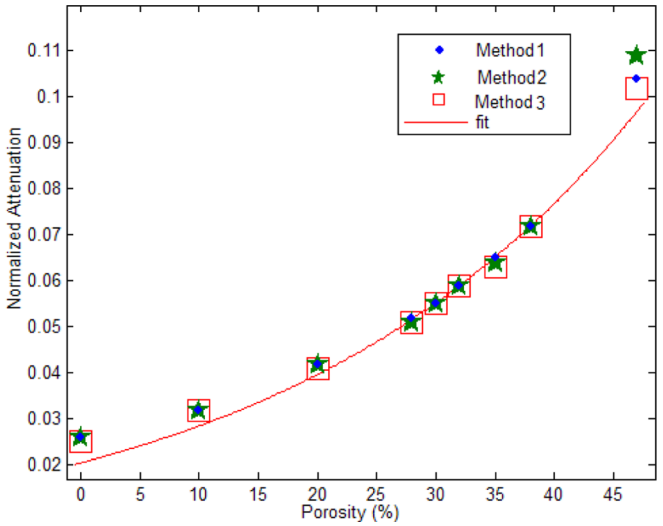

FIG. 3. Variation of normalized attenuation coefficient versus porosity for the three methods.

Figure 3 shows the same variation for average value of constants. Therefore, the shape of the curve follows a variation of the form: $\alpha_N = 0.0217\exp(3.162P)$.

It is well established that the transducer converted an electrical signal into an acoustic signal of the same frequency. The resolution of an acoustic microscope is better when this frequency is high. In order to quantify the influence of the sensor's vibration frequency on the absorption of the Rayleigh wave, α_R, in PSi, we calculated α_R at different frequencies that vary from 58 to 650 MHz. The evolution of α_R versus frequency is shown in 3D in Fig. 4. The latter also shows the variation of the Rayleigh attenuation versus porosity. Note that these variations are the average of the values obtained by the three methods. In this case, the following observations can be made:

– For a given material, when the frequency increases, the attenuation also increases.
– At a given frequency, the attenuation is even stronger when the Rayleigh attenuation is great.

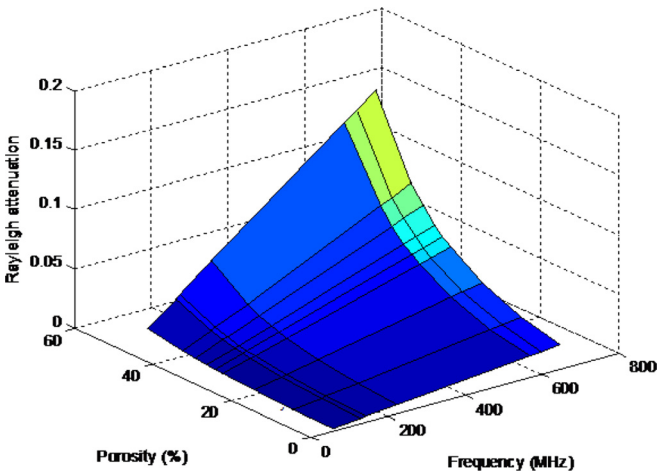

FIG. 4. 3D presentation of the variation of Rayleigh attenuation versus the porosity and the frequency in the case water/PSi structure.

– The evolution of the attenuation versus the frequency is practically linear with a characteristic slope of the material.

To overcome the divergences of linear inclination—in other words, to generalize the dependence frequency-attenuation at any value of porosity, curves in Fig. 3 allow us to obtain, by fitting the equations of the form

$$\alpha_R = A \cdot f,$$

with $A = A_0 (1\text{-}P)^{m}$, where $A_0 = 3.154\ 10^{-5}$ and $m = -3.28$.

IV. CONCLUSION

The dependence of such attenuation coefficients on porosities as well as on operating frequencies by using different methods was then investigated to establish empirical relations between these parameters. The obtained values of attenuation coefficients are in a good concordance, which can be applied to several porous materials and to predict the interdependence between different parameters.

[1]Y. C. Lee Jan, D. Achenbach, J. O. Kim, and Y. C. Lee, IEEE Ultrason. Symp. **1**, 607 (1993).
[2]J. I. Kushibiki, M. Arakawa, S. Yoshida, and K. Otsu, IEEE International Ultrason. Symp. Proc., 611 (2008).
[3]P. Zinin, O. Lefeuvre, G. A. D. Briggs, B. D. Zeller, P. Cawley, A. J. Kinloch, and G. E. Thompson, J. Appl. Phys. **82**, 1031 (1997).
[4]I. A. Viktorov, *Rayleigh and Lamb Waves* (Plenum, New York, 1967), p. 46.
[5]J. Kushibiki, Y. Matsumoto, and N. Chubachi, IEEE Ultrasonic Symp. Proc., 610 (1984).
[6]S. Bouhedja, I. Hadjoub, A. Doghmane, and Z. Hadjoub, Phys. Status Solidi A **202**, 1025 (2005).
[7]G. A. D. Briggs and O. V. Kolosov, *Acoustic Microscopy*, 2nd ed. (New York, Oxford University Press, 2010).
[8]C. G. R. Sheppard and T. Wilson, Appl. Phys. Lett. **38**, 858 (1981).
[9]M. J. Sailor, *Porous Silicon in Practice* (Wiley-VCH, Weinheim, 2012).
[10]D. Bellet, in *Properties of Porous Silicon*, edited by L. Canham (INSPEC, London, 1997).
[11]G. T. Andrews, A. M. Polomska, E. Vazsonyi, and J. Volk, Phys. Status Solidi A **204**, 1372 (2007).
[12]G. N. Aliev, B. Goller, and P. A. Snow, J. Appl. Phys. **110**, 043534 (2011).
[13]L. C. Parsons and G. T. Andrews, J. Appl. Phys. **111**, 123521 (2012).
[14]R. J. M. da Fonseca, J. M. Saurel, G. Despaux, A. Foucaran, E. Massonne, T. Taliercio, and P. Lefebvre, Superlattices Microstruct. **16**, 21 (1994).
[15]R. J. M. Da Fonseca, J. M. Saurel, A. Foucaran, J. Camassel, E. Massone, T. Taliercio, and Y. Boumaiza, J. Mater. Sci. **30**, 35 (1995).
[16]Y. Boumaiza, A. Hadjoub, A. Doghmane, and L. Deboub, J. Mater. Sci. Lett. **18**, 295 (1999).
[17]Y. C Lee, J. O. Kim, and J. D. Achenbach, IEEE Trans. Ultrason. Ferroelectr. Freq. Control **42**, 253 (1995).
[18]J. Kushibiki and N. Chubachi, IEEE Trans. Sonics Ultrason. **32**, 189 (1985).
[19]W. Parmon and H. L. Bertoni, Electron. Lett. **15**, 684 (1979).
[20]A. Doghmane and Z. Hadjoub, J. Phys. D: Appl. Phys. **30**, 2777 (1997).
[21]S. Bouhedja, I. Hadjoub, A. Doghmane, and Z. Hadjoub, J. Optoelec. Adv. Mater. Symp. **1**, 420 (2009).
[22]R. J. M. Da Fonseca, J. M. Saurel, A. Foucaran, E. Massone, T. Taliercio, and J. Camassel, Thin Solid Films **255**, 155 (1995).